1979 International Symposium on lepton and photon interactions at high energies.
Batavia, USA, August 23 - 29, 1979.
CEA - CONF 5003

FR 8001611

INIS

POSSIBLE OBSERVATION OF A MESON AT 5.3 GeV/c^2

R. Barate*), P. Bareyre, P. Bonamy, P. Borgeaud, M. David, J. Ernwein**), F.X. Gentit, G. Laurens, Y. Lemoigne, A. Roussarie†), G. Villet and S. Zaninotti
Centre d'Etudes nucléaires, Saclay, Gif-sur-Yvette, France

P. Astbury, A. Duane, G.J. King, B.C. Nandi, D.P. Owen**), D. Pittuck, D.M. Websdale, J. Wiejak, W.C.S. Williams†) and A. Wylie*)
Imperial College, London, England

J.G. McEwen
Southampton University, England

M.A. Abolins**), B. Brabson, R. Crittenden, R. Heinz, J. Frider, T. Marshall and T. Palfrey††)
Indiana University, Bloomington, Indiana, USA

ABSTRACT

We report on π^-N events observed at 150 and 175 GeV/c in a large-acceptance spectrometer triggered by $J/\psi \to \mu\mu$. We observe with high mass-resolution the particles ψ', Σ^0 and Λ. We present evidence for a new resonance at 5.3 GeV/c^2, whose possible interpretation is a meson containing a b-quark.

* * *

At the CERN Super Proton Synchrotron (SPS) we have performed an experiment which was designed to look at the hadrons associated with lepton pairs produced in π^-Be scattering at 150 and 175 GeV/c.

A side view of the apparatus is shown in Fig. 1. The apparatus is composed of a 18.8 g cm^{-2} Be target (split into three parts to minimize γ conversions) placed in front of a vertex spectrometer. In the forward direction the set-up is "completed" by a lever-arm spectrometer equipped with a multicellular Čerenkov counter and a muon identifier.

The vertex spectrometer consists of the Goliath magnet (1.5 T, Ø pole 2 m, gap 1.05 m), whose centre is 2.25 m from the middle target; Goliath is filled with two small proportional chambers (0.6 × 0.22 m^2; one vertical plane, 1 mm wire spacing; two tilted planes, 2 mm wire spacing) and eleven medium-sized proportional chambers (1.8 × 7 m^2; four planes, 2 mm wire spacing). The number of wires in Goliath is ≈ 30,000.

The forward lever-arm is composed of two large proportional chambers (3 × 2 m^2, four planes, 3 mm wire spacing) and a multicellular (28 cells) Čerenkov counter filled with CO_2 at atmospheric pressure. The muon filter consists of an iron shield, 3.4 m thick, sandwiched between horizontal slabs of scintillator. The front and rear slabs are arranged in pairs which point forward the targets. The pairs are combined to define four quadrants relative to the median horizontal and vertical planes of the experiment (each quadrant has eight pairs of slabs). A vertical hodoscope (40 slabs) completes the muon identification after the iron.

The trigger is based on the detection of opposite-sign muons; this is achieved by requiring hits in either pair of the diagonally opposite quadrants. A gap in the horizontal median plane of ±16 mrad is provided in order to lower the trigger rate coming from π-μ decays, between the target and the muon filter, which produce mainly low $\mu\mu$ effective masses. The J/ψ production rate is 0.35×10^{-3} (≈ 100 J/ψ/day).

RESULTS

1. IDENTIFICATION OF KNOWN PARTICLES

Figure 2 shows the J/ψ and ψ' signal obtained without any renormalization of the magnetic field map. One gets

				Tables:
$m_{J/\psi}$	= 3095.44	± 0.46	MeV/c^2	3097 ± 2
$m_{\psi'}$	= 3683	± 6	MeV/c^2	3684 ± 3
$\sigma_{J/\psi}$	= 37.5	± 0.4	MeV/c^2	
$\sigma_{\psi'}$	= 35	± 6	MeV/c^2	

The fit of the full spectrum with two exponentials for the background and two Gaussians for the J/ψ and ψ' shows that out of 10,640 events between 2.95 and 3.25 GeV/c^2 there are 9000 J/ψ's. (This spectrum excludes a sample of 1650 J/ψ's taken with a special $\chi \to J/\psi\,\gamma$-detector configuration.) The background in our J/ψ sample is thus about 15%.

---

*) Present address: CERN, Geneva, Switzerland.
**) Present address: Michigan State University, East Lansing, Michigan, USA.
†) Present address: SLAC, Stanford, Calif., USA.
††) On leave from Purdue University, West Lafayette, Indiana, USA.

One gets also 140 ψ''s with a background of about 40% in the 3.585-3.785 GeV/c^2 mass range. The mass resolution [$\sigma(M)/M = 1.2\%$] is far better than for a beam dump experiment and allows a clear separation of the J/ψ and ψ' peaks.

Figure 3 presents the $J/\psi\,\pi\pi$ effective mass spectrum. The ψ' signal appears in spite of the high combinatorial background. The background shape is obtained by a polynomial fit to the $J/\psi\,\pi^+\pi^+ + J/\psi\,\pi^-\pi^-$ distribution. The solid line is the fit obtained with a Gaussian for the resonance plus the previously determined polynomial fit of the background. We get

$$M = 3682 \pm 2 \text{ MeV},$$

$$\sigma = 12 \pm 4 \text{ MeV}.$$

The peak contains 280 events. To obtain such a good resolution, the J/ψ mass has been constrained to take its exact value[1].

2. ASSOCIATED PARTICLES

Figure 4a gives the π^- effective mass spectrum versus the $p\pi$ effective mass spectrum for the V^0's collected in our experiment. The Λ and the K^0 signals and the γ reflection can clearly be seen. Figure 4b gives the e^+e^- effective mass spectrum versus the $\pi\pi$ one for the same V^0's. Here the K^0, the γ, and the Λ reflection can be seen.

In what follows, we reject the areas of Fig. 4 which contain the ambiguities between K^0 and γ, between K^0 and Λ, and between Λ and γ. Figure 5a shows the K^0 signal. A fit to the mass gives

		Tables:
M_{K^0} =	497.74 ± 0.45 MeV/c^2	497.67 ± 0.13
σ =	8.1 ± 0.4 MeV/c^2.	

It yields 520 ± 28 K^0's out of a total of 660 events in a ±20 MeV/c^2 mass range centred on 498 MeV/c^2. Hence for the events in this range, the background is 21%. Figure 5b shows the $\Lambda + \bar{\Lambda}$ signal. A fit to the mass distribution gives

		Tables:
M_Λ =	1115.3 ± 0.2 MeV/c^2	1115.6 ± 0.05
σ =	2.6 ± 0.3 MeV/c^2.	

This yields 180 ± 20 Λ's.

3. $J/\psi\,K\pi$ EFFECTIVE MASSES

Building $J/\psi\,K$, $J/\psi\,K^*$, $J/\psi\,K\pi$, $J/\psi\,K^*$: effective mass spectra is a way of looking for possible naked beauty states; a possible quark diagram is:

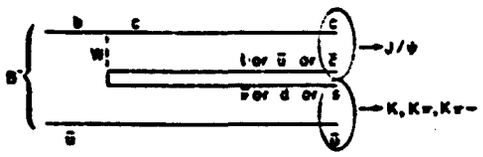

One expects masses greater than 5.2 GeV/c^2 due to the limit set by the Υ'':

$$M_B > \frac{M_{\Upsilon''}}{2} = 5.2 \text{ GeV}/c^2$$

Our sample of 9000 J/ψ's is composed of two subsets: one (6671 J/ψ's) taken at 150 GeV/c, and the other (2324 J/ψ's) taken at 175 GeV/c incident pion momentum. The $J/\psi\,K^0\pi^\pm$ effective mass spectrum is given for both samples combined in Fig. 6. In each effective mass calculation the J/ψ and K^0 are constrained to their exact value[1]. The binning, 40 MeV, is equal to the resolution. A peak shows up at 5.3 GeV/c^2. The $J/\psi\,K^-\pi^+$ spectrum seen in Fig. 7 also shows an enhancement at 5.3 GeV/c^2. It appears clearly when we ask for $p_T(K) > 0.5$ GeV/c. The $J/\psi\,K^+\pi^-$ spectrum does not show anything (Fig. 8), but it can be seen that the background is twice that for the K^-; it is probably due to the proton contamination of our K^+ sample. Figure 9 shows the sum of the $J/\psi\,K^0\pi^\pm$ and $J/\psi\,K^-\pi^+$ channels: in Fig. 9a with 40 MeV bins and in Fig. 9b with 20 MeV bins. A fit to the spectrum with a polynomial plus a Gaussian yields

$$M_B = 5300 \pm 7 \text{ MeV}/c^2$$

$$\sigma = 22 \pm 7 \text{ MeV}/c^2$$

$$N = 45 \pm 14$$

In order to estimate the statistical significance of this peak, we have made a special histogram in which a given event contributes only once to a given bin (Fig. 9c). We get:

Signal	25 events
Background	37 events
Total	62 events
$S/\sqrt{B}$ =	4.1 σ
$S/\sqrt{T}$ =	3.1 σ

3.1 Cross-section estimate for $\pi^- p \to B\bar{B} + X$

Our average J/ψ total production cross-section is 100 ± 10 nb[2]. With 9000 J/ψ's there is a sensitivity of ~ 11 pb/$J\psi$ event. Without any established production model it is difficult to estimate our acceptance. A crude calculation for the K acceptances leads to $B\sigma \sim$ ~ 2 nb.

If the branching ratio is around 1% [1], we get $\sigma_{B\bar{B}} \sim 200$ nb. This result is not far from previously predicted cross-sections [2].

3.2 Theoretical interpretation

In March 1979, Fritzsch [3] predicted observable decays of the B in J/ψ K, J/ψ K^*, J/ψ Kπ, J/ψ $K^*\pi$. The branching fractions at each vertex that he predicts are:

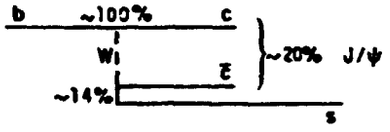

This leads to an estimate of the branching fraction $B \to J/\psi$ X of $\sim$ 3%. We do not see anything in J/ψ K and J/ψ K^*.

Since then, Fritzsch [3] and Wetzel (private communication) have given kinematical arguments which suppress the J/ψ K and J/ψ K^* modes: since the recoiling invariant mass is between 1.1 and 1.8 GeV/c, the J/ψ Kπ mode is favoured.

4. A SECOND WAY OF LOOKING FOR BEAUTY

An alternative diagram which also has J/ψ, K's, and π's in the final state is:

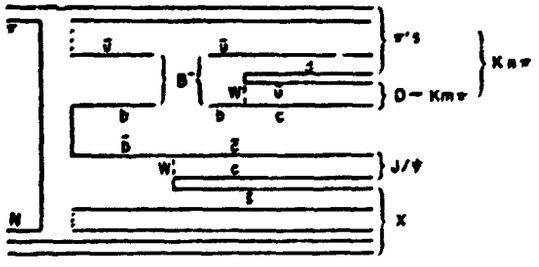

In this, a B meson decays to Dπ, D2π, ...

Summing all channels $(K^{\pm} m\pi^{\pm})^{\pm}$ with $2 \leq n \leq 5$, we get Fig. 10a. No peak appears. If we ask that one combination $(K^{\pm} m\pi^{\pm})^{\pm}$ with $1 \leq m \leq n-1$ has the mass ($M_D \pm 40$ MeV) we get Fig. 10b. A small peak appears at 5.3 GeV/c^2. An additional cut on the $K^{\pm}$, $K^{\pm}$ transverse momentum, $p_T(K) > 0.5$ GeV/c, reinforces the signal (Fig. 10c); this cut is justified because a heavy mass decays into light particles.

The peak is still there (Fig. 11) if we restrict the mass $(K^{\pm} m\pi^{\pm})^{\pm}$ further to be $M_D \pm 20$ MeV.

CONCLUSION

Evidence for a new resonance at 5.3 GeV/c^2 is appearing. In the J/ψ Kπ channel there is a 4.1σ effect; in the K nπ channels an effect is also seen. Clearly, more statistics are needed in order to settle the question. The reason why it seems easier to see the B than the D signal, despite the small branching ratio in both cases, is that the J/ψ, the trigger particle, enters the effective mass combination, whereas this is not the case for the D. Moreover, the J/ψ, with its very clear signature, allows us to reach very small cross-sections. For the K nπ case, because of the large mass of the B, the signal appears because there is little phase-space left for the background and because we sum all the possible K mπ decays of the D.

REFERENCES

1) Particle Data Group, Phys. Lett. 75B (1978).

2) M. Abolins et al., Phys. Lett. 82B, 145 (1979).

3) H. Fritzsch, CERN preprint TH 2648 (March 1979).

4) H. Fritzsch and K. Streng, Phys. Lett. 78B, 447 (1979).

5) H. Fritzsch, CERN preprint TH 2703 (July 1979).

FIGURE CAPTIONS

Fig. 1 Experimental layout. H represents a scintillator hodoscope; μ is a muon beam halo detector.

Fig. 2 Dimuon mass spectrum, uncorrected for geometrical acceptance.

Fig. 3 $J/\psi\ \pi^+\pi^-$ mass spectrum with the background shape from $J/\psi\ \pi^+\pi^+ + J/\psi\ \pi^-\pi^-$ superimposed.

Fig. 4a $p\pi$ effective mass spectrum versus the $\pi\pi$ effective mass spectrum for the observed V^0's.

Fig. 4b $\pi^+\pi^-$ effective mass spectrum versus the e^+e^- effective mass spectrum for the same V^0's.

Fig. 5a Mass spectrum of the K^0.

Fig. 5b Mass spectrum of the Λ and $\bar{\Lambda}$.

Fig. 6 $J/\psi\ K^0\pi^\pm$ effective mass spectrum.

Fig. 7 $J/\psi\ K^-\pi^+$ effective mass spectrum with $p_T(K^-) > 0.5$ GeV/c.

Fig. 8 $J/\psi\ K^+\pi^-$ effective mass spectrum with $p_T(K^+) > 0.5$ GeV/c.

Fig. 9a A sum of the $J/\psi\ K^0\pi^\pm$ and $J/\psi\ K^-\pi^+$ effective mass spectra, with 40 MeV/c^2 bins.

Fig. 9b Same as (a), with 20 MeV/c^2 bins.

Fig. 9c $J/\psi\ K^0\pi^\pm$ effective mass spectrum in which an event contributes only once to a given bin.

Fig. 10 $(K^\pm n\pi^\pm)^\pm$ effective mass spectrum:

a) $2 \le n \le 5$;

b) Same as (a) with the additional requirement that the effective mass $(K^\pm m\pi^\pm)^\pm$ has the mass ($M_D \pm$ $\pm$ 40 MeV/c^2) and $1 \le m \le n-1$;

c) Same as (b) with $p_T(K) > 0.5$ GeV/c.

Fig. 11 Same as Fig. 10 but with mass $(K^\pm m\pi^\pm)^\pm = M_D \pm 20$ MeV/c^2.

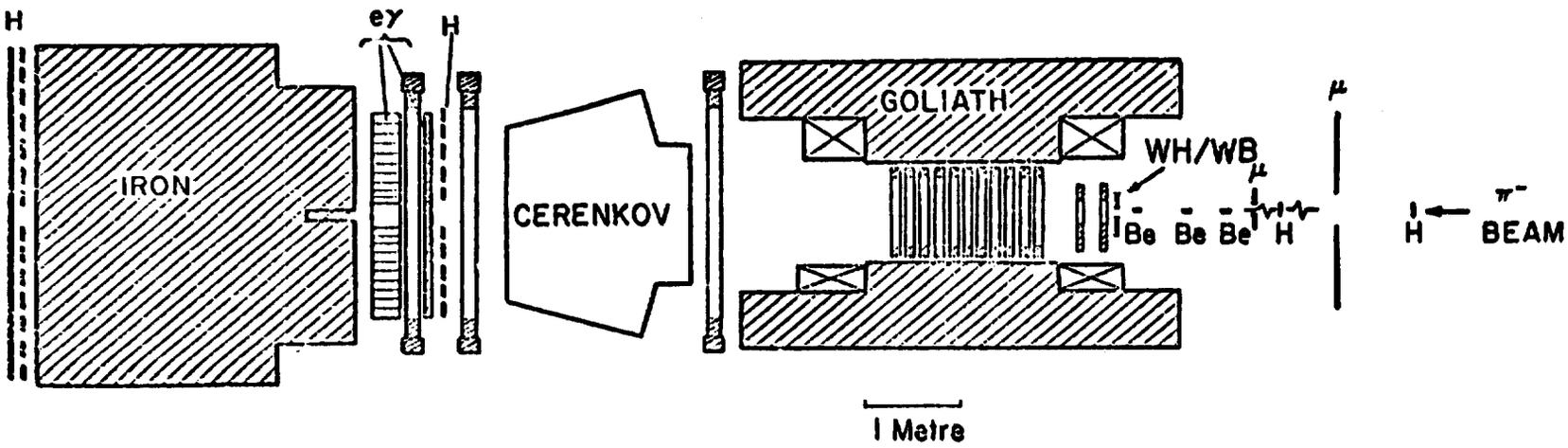

FIG. 1

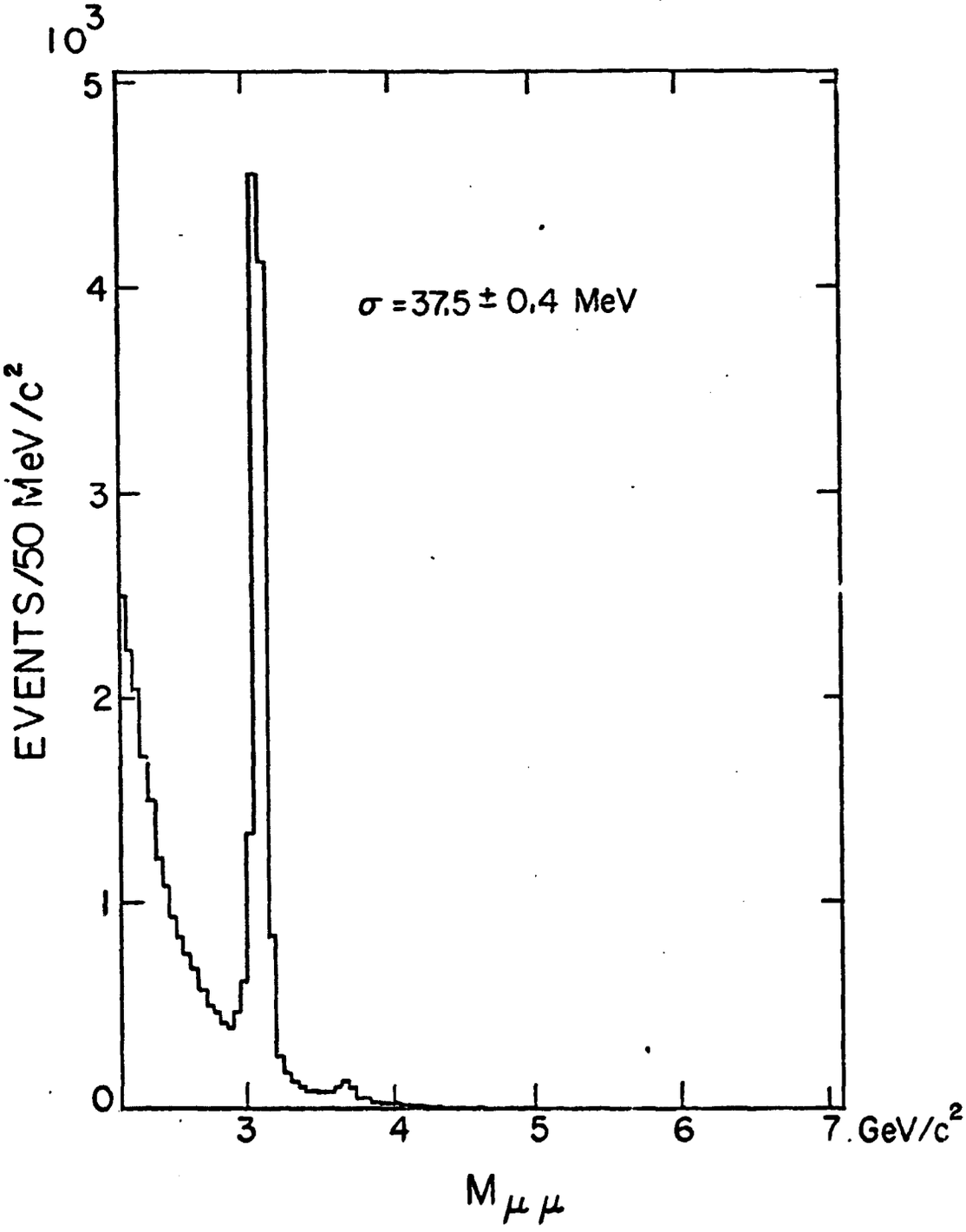
10^3
5
4
3
2
1
0
EVENTS/50 MeV/c^2
$\sigma = 37.5 \pm 0.4$ MeV
3
4
5
6
7 GeV/c^2
$M_{\mu\mu}$

FIG. 2

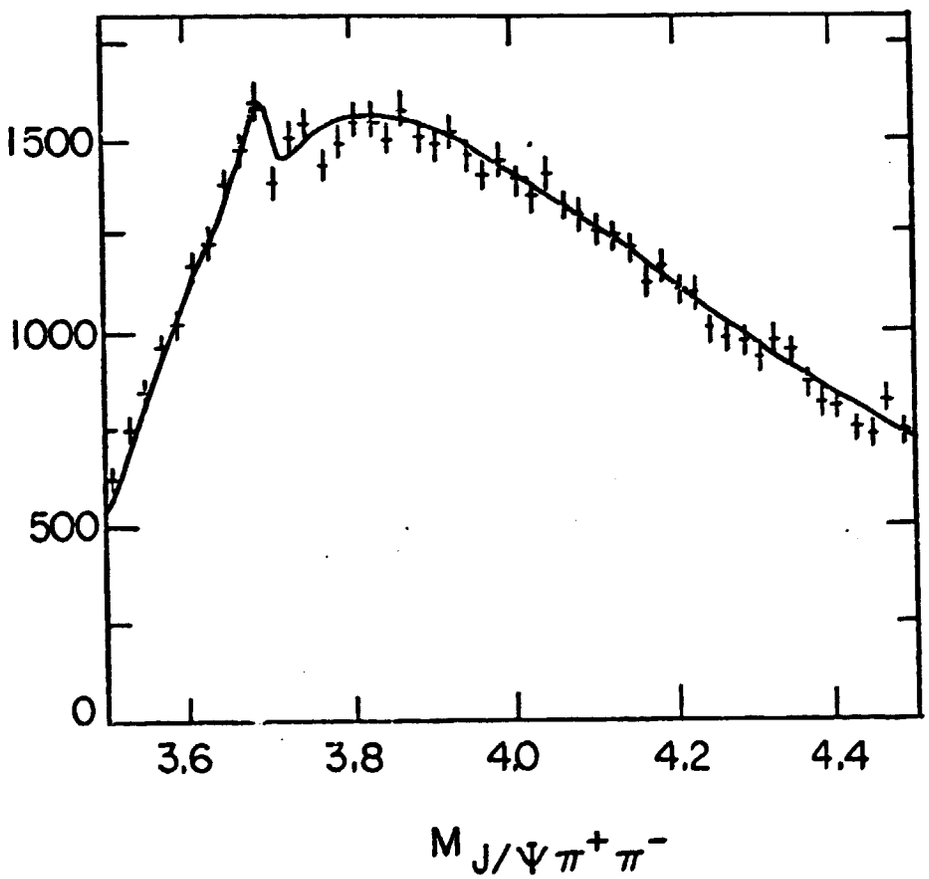

FIG. 3

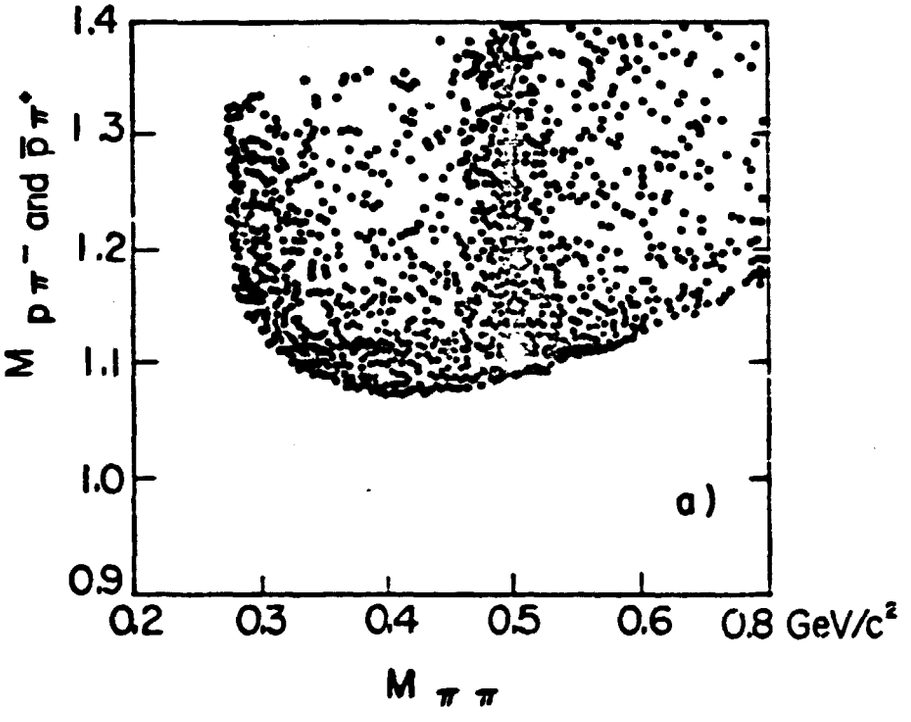
1.4
1.3
1.2
1.1
1.0
0.9
M p π⁻ and p̄ π⁺
a)
0.2
0.3
0.4
0.5
0.6
0.8 GeV/c²
M π π

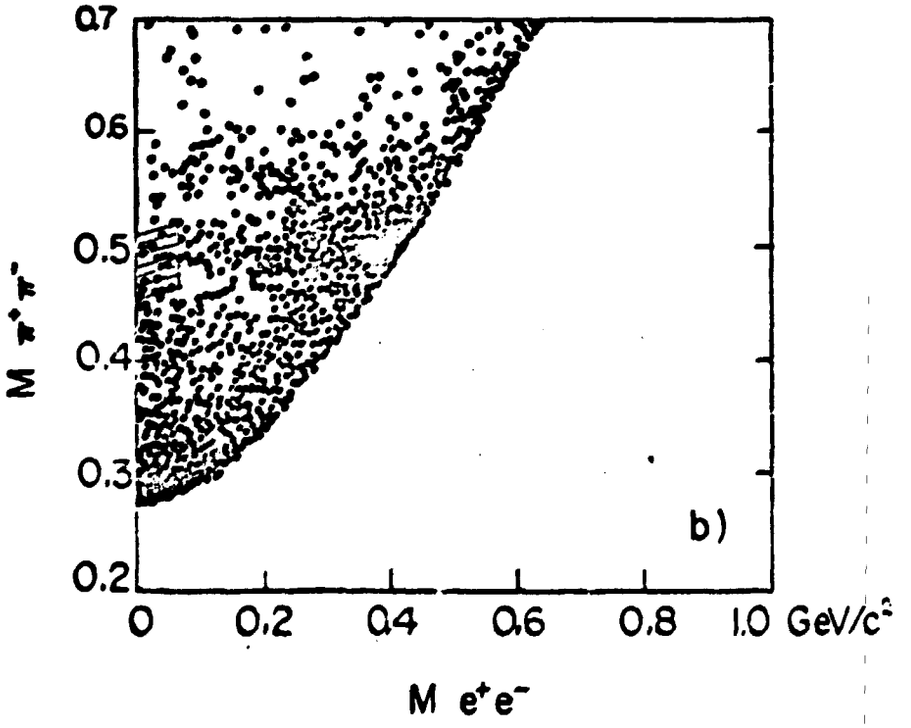
0.7
0.6
0.5
0.4
0.3
0.2
M π⁺π⁻
b)
0
0.2
0.4
0.6
0.8
1.0 GeV/c²
M e⁺e⁻

FIG. 4

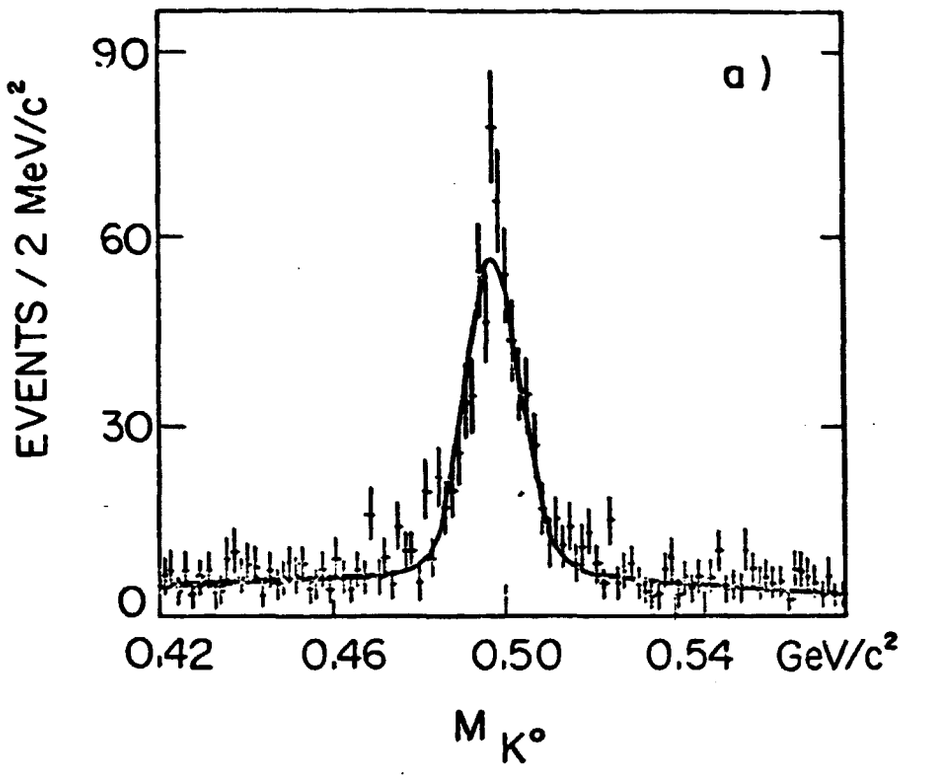
a)
90
60
30
0
EVENTS / 2 MeV/c²
0.42
0.46
0.50
0.54
GeV/c²
M K°

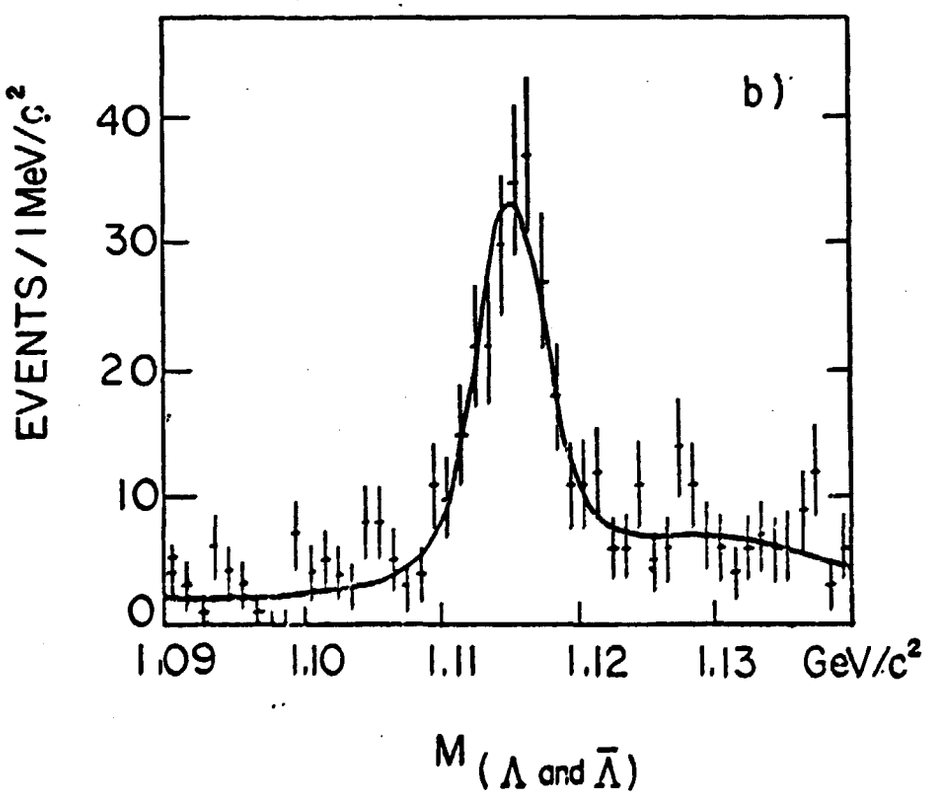
b)
40
30
20
10
0
EVENTS / 1 MeV/c²
1.09
1.10
1.11
1.12
1.13
GeV/c²
M (Λ and Λ̄)

FIG. 5

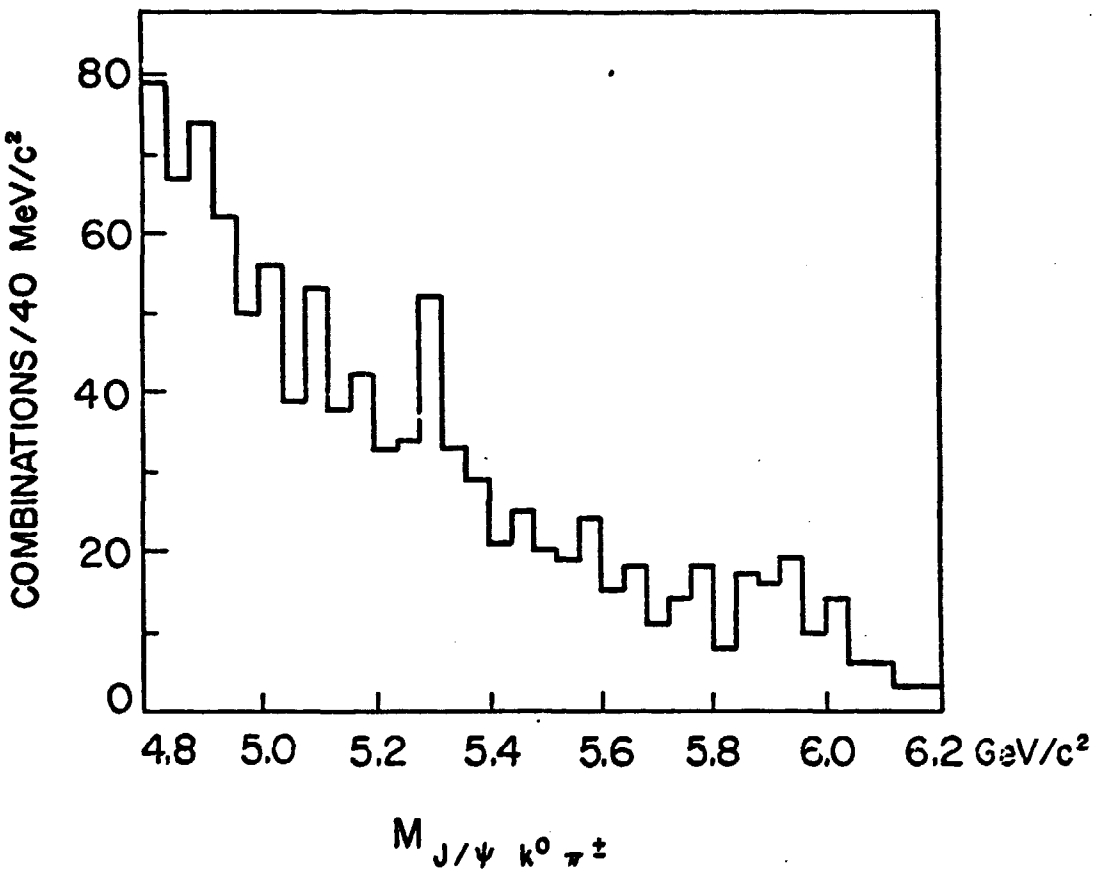
80
60
40
20
0
COMBINATIONS/40 MeV/c²
4.8
5.0
5.2
5.4
5.6
5.8
6.0
6.2 GeV/c²
M J/ψ k⁰ π±

FIG. 6

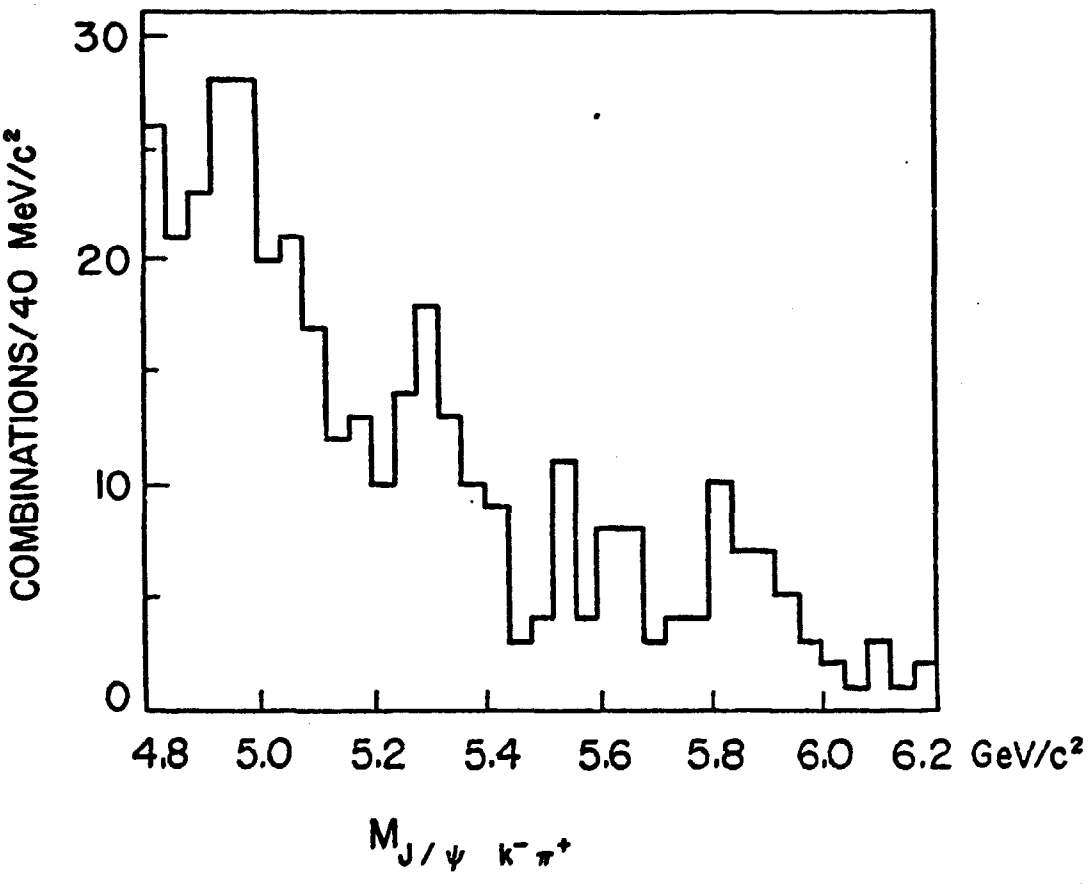
30
20
10
0
COMBINATIONS/40 MeV/c²
4.8
5.0
5.2
5.4
5.6
5.8
6.0
6.2 GeV/c²
M J/ψ k⁻π⁺

FIG. 7

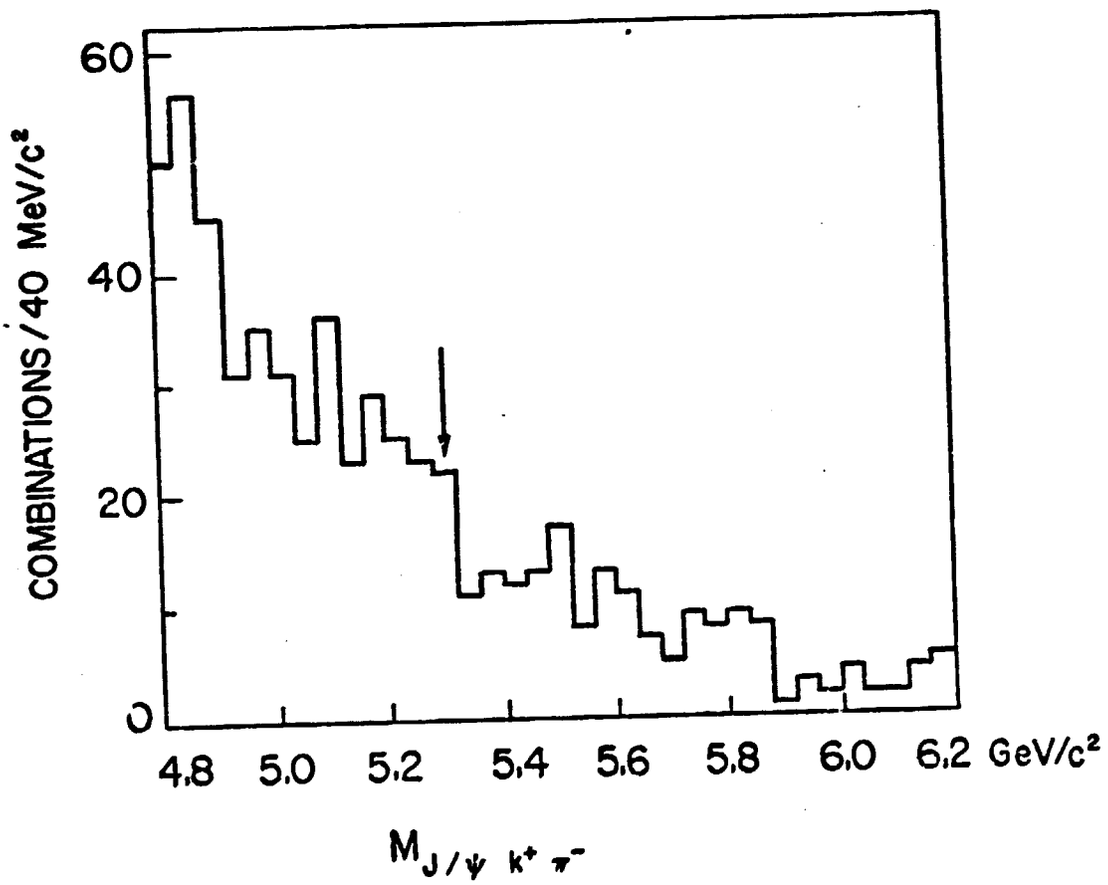
60
40
20
0
COMBINATIONS/40 MeV/c²
4.8
5.0
5.2
5.4
5.6
5.8
6.0
6.2 GeV/c²
M J/ψ k⁺ π⁻

FIG. 8

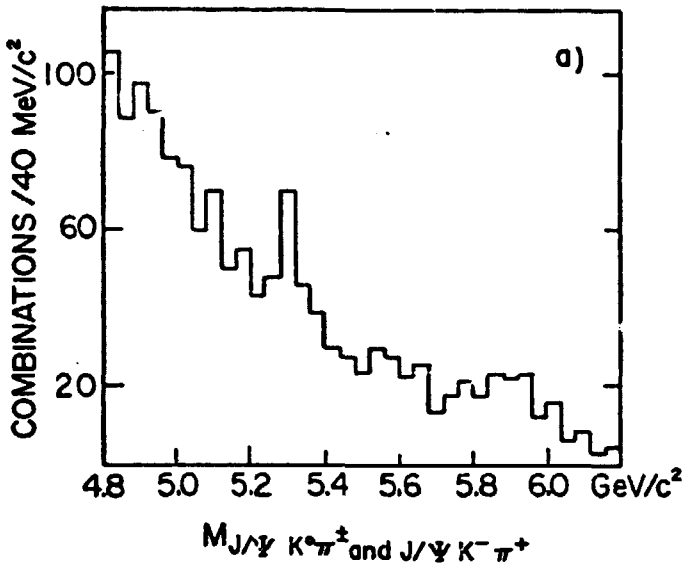
a)
COMBINATIONS /40 MeV/c²
100
60
20
4.8 5.0 5.2 5.4 5.6 5.8 6.0 GeV/c²
M J/Ψ K°π± and J/Ψ K⁻π⁺

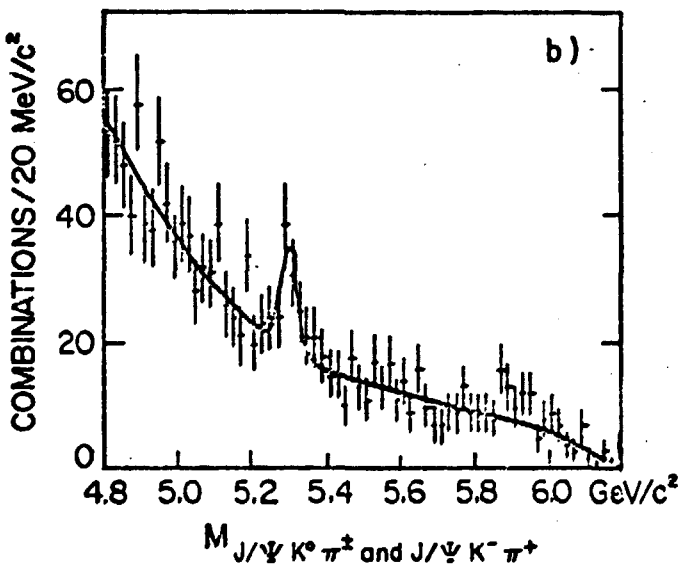
b)
COMBINATIONS/20 MeV/c²
60
40
20
0
4.8 5.0 5.2 5.4 5.6 5.8 6.0 GeV/c²
M J/Ψ K°π± and J/Ψ K⁻π⁺

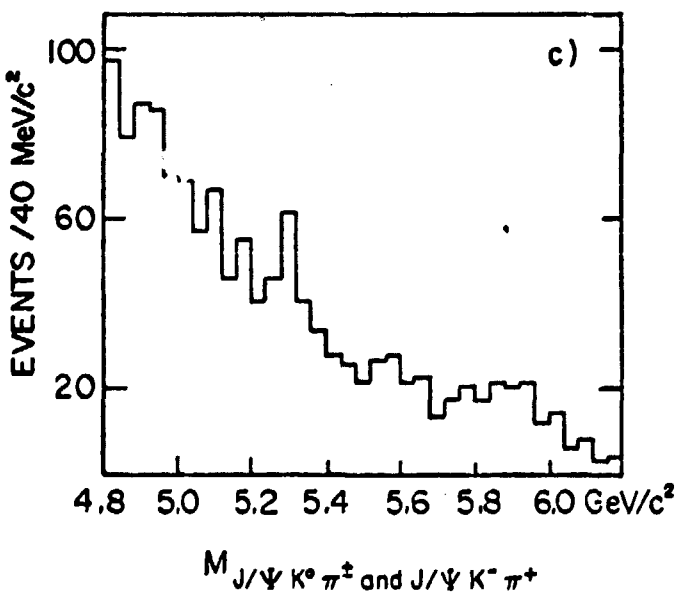
c)
EVENTS /40 MeV/c²
100
60
20
4.8 5.0 5.2 5.4 5.6 5.8 6.0 GeV/c²
M J/Ψ K°π± and J/Ψ K⁻π⁺

FIG. 9

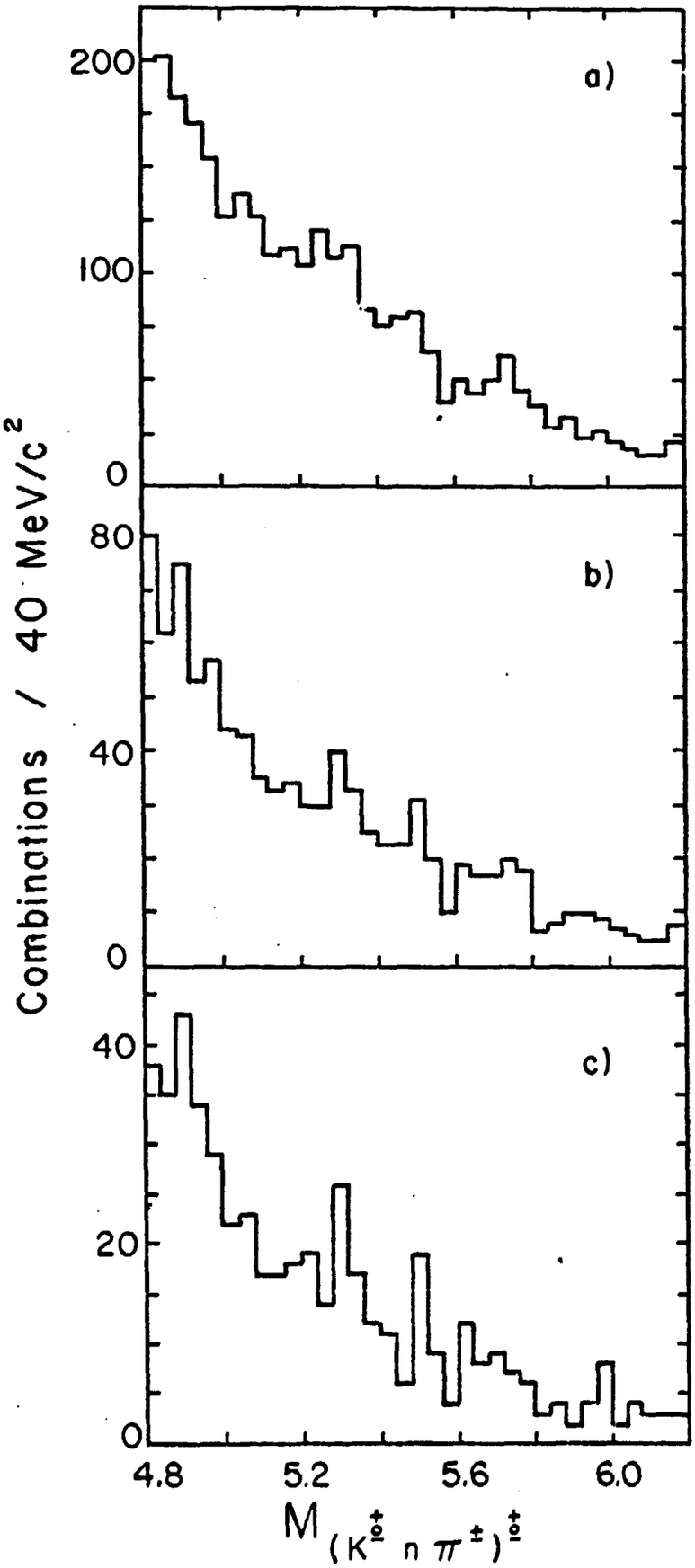
a)
b)
c)
200
100
0
80
40
0
40
20
0
4.8
5.2
5.6
6.0
Combinations / 40 MeV/c²
M(K± n π±)±

FIG. 10

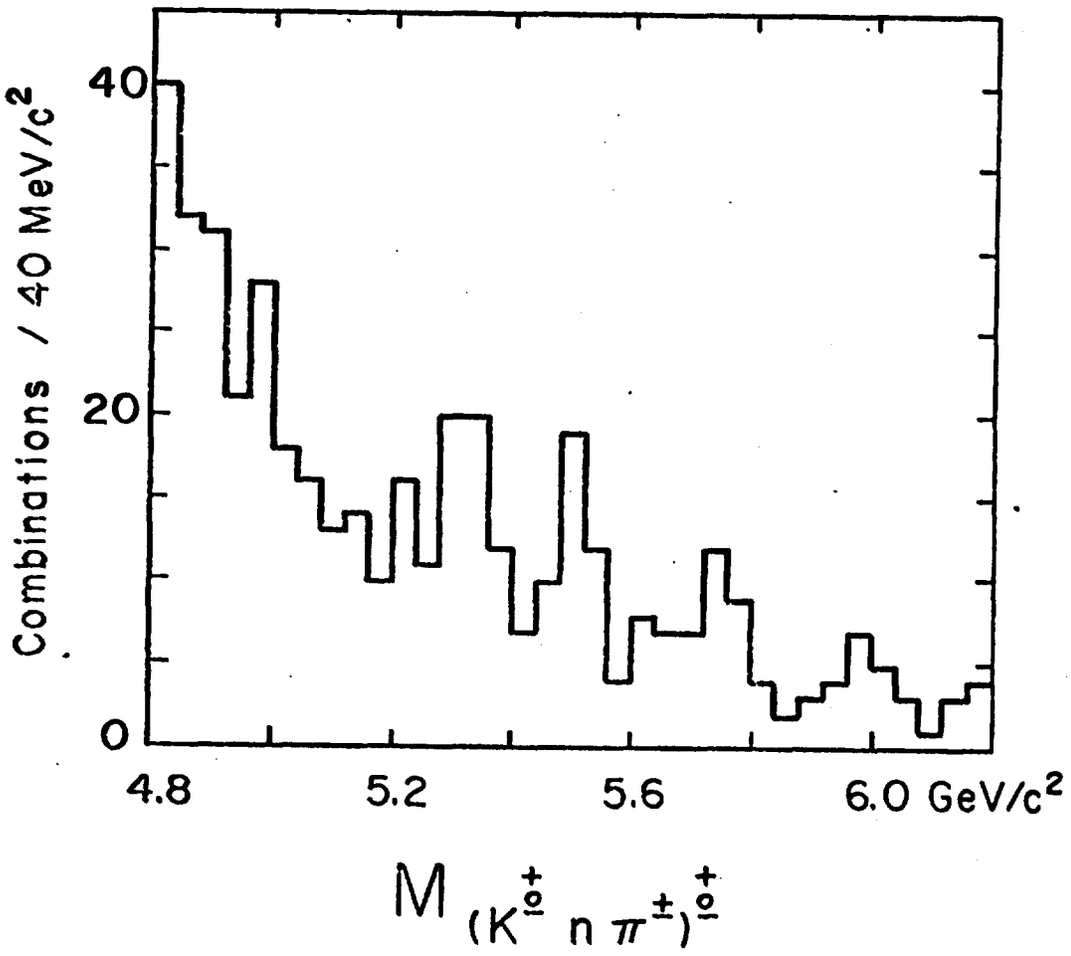

FIG. 11